Eur. Phys. J. B **17**, 235–243 (2000)

THE EUROPEAN PHYSICAL JOURNAL B

EDP Sciences

d-wave nonadiabatic superconductivity

P. Paci[1,a], C. Grimaldi[2], and L. Pietronero[1]

[1] INFM Unitá di Roma 1 and Dipartimento di Fisica, Università di Roma 1 "La Sapienza", Piazzale A. Moro 2, 00185 Roma, Italy
[2] École Polytechnique Fédérale de Lausanne, DMT-IPM, 1015 Lausanne, Switzerland

Received 12 May 2000

Abstract. The inclusion of nonadiabatic corrections to the electron-phonon interaction leads to a strong momentum dependence in the generalized Eliashberg equations beyond Migdal's limit. For a s-wave symmetry of the order parameter, this induced momentum dependence leads to an enhancement of T_c when small momentum transfer is dominant. Here we study how the d-wave symmetry affects the above behavior. We find that the nonadiabatic corrections depend only weakly on the symmetry of the order parameter provided that only small momentum scatterings are allowed for the electron-phonon interaction. In this situation, We show that also for a d-wave symmetry of the order parameter, the nonadiabatic corrections enhance T_c. We also discuss the possible interplay and crossover between s- and d-wave depending on the material's parameters.

PACS. 63.20.Kr Phonon-electron and phonon-phonon interactions – 71.38.+i Polarons and electron-phonon interactions – 74.20.Mn Nonconventional mechanisms

1 Introduction

In ordinary low-temperature superconductors, the smallness of the relevant phonon frequency ω_0 compared to the Fermi energy E_F permits to formulate a theory of superconductivity based on a closed set of formulas known as Migdal-Eliashberg (ME) equations [1,2] allowing quantitative agreements with experiments [3]. The closed form of the ME equations stems from Migdal's theorem which states that as long as $\omega_0/E_F \ll 1$ the electron-phonon (e-ph) vertex corrections to the electron self-energy are at least of order $\lambda\omega_0/E_F$, where λ is the e-ph coupling, and can therefore be neglected [1].

A different situation is encountered in high-T_c superconductors such as cuprates and fullerides. These materials have in fact Fermi energies much smaller than those of conventional metals [4,5] so that the energy scale ω_0 associated to the mediator of the superconducting pairing can be comparable to E_F. Hence, the quantity ω_0/E_F is no longer negligible and in principle vertex corrections become relevant preventing the ordinary ME scheme to be a correct description of the superconducting state.

The possible breakdown of Migdal's theorem in high-T_c superconductors inevitably calls for a generalization beyond the ME scheme to include the no longer negligible vertex corrections. A possible way to accomplish this goal is to rely on a perturbative scheme by truncating the infinite set of vertex corrections at a given order. In previous works, we have proposed a perturbative scheme in which the role of small parameter is played roughly by $\lambda\omega_0/E_F$ leading to a generalized ME theory which includes the first nonadiabatic vertex corrections [6,7]. For a single-electron Holstein model, such a first order perturbative approach leads to good agreements with exact results as long as the system is away from polaron formation, that is for $\lambda < \lambda_c \simeq 1$ [8]. The region of validity of the perturbative approach, which we could name nonadiabatic region, is characterized by quasi-free electrons ($\lambda < 1$) coupled in a nonadiabatic way (ω_0/E_F not negligible) to the lattice. According to this definition, our nonadiabatic region is different from the classic polaronic picture. Of course, larger values of λ would render higher order vertex corrections important leading to the breakdown of our truncation scheme.

The key point of the nonadiabatic theory, is that the e-ph effective interaction is described in terms of vertex corrections which depend on the momentum transfer $|\mathbf{q}| = q$ and the Matsubara exchanged frequency ω in a non-trivial way. For example, the e-ph vertex correction appearing in the normal state self-energy becomes positive (negative) when $v_F q < \omega$ ($v_F q > \omega$), where v_F is the Fermi velocity [7]. The generalization to the superconducting transition reveals that this situation is also encountered for the class of diagrams beyond Migdal's limit relevant for the Cooper channel. Concerning the critical temperature T_c, as long as the momentum transfer is less than ω_0/v_F, the nonadiabatic corrections lead to a strong enhancement of T_c also for moderate values of the e-ph coupling λ [6,7,9]. Such a strong momentum-frequency

[a] e-mail: paola@pil.phys.uniroma1.it

dependence of the vertex corrections is confirmed by numerical calculations within a tight-binding approach [10] and general theoretical considerations on the physical interpretation of such nonadiabatic corrections [11].

So far, nonadiabatic superconductivity has been studied by requiring the order parameter Δ to be independent of the momenta. This situation is certainly suitable for the fullerene compounds which are s-wave superconductors. However, one striking characteristic of several high-T_c superconductors is the strong momentum dependence of the order parameter $\Delta(\mathbf{k})$. Among the several types of measurements aimed to resolve the pairing symmetry, the Josephson tunneling [12] and angle resolved photoemission experiments [13] are the most convincing ones showing that the order parameter of several cuprates, maybe with the exception of the electron-doped NCCO, has a predominant d-wave symmetry: $\Delta(\mathbf{k}) \simeq \Delta[\cos(k_x) - \cos(k_y)]$.

The origin of the d-wave symmetry in high-T_c cuprates is still debated. On one hand, the observed d-wave symmetry is regarded as an evidence against any purely electron-phonon pairing interaction so that the mechanism responsible for superconductivity should be sought among pairing mediators of electronic origin (like antiferromagnetic fluctuations) with eventually a minor electron-phonon component. On the other hand, several theoretical studies have shown that the e-ph interaction could produce, under some quite general circumstances, a d-wave symmetry of the condensate [14,15]. This could happen when for example charge carriers experience an on-site repulsive interaction together with a phonon induced attraction for large inter-electrons distances. The on-site repulsion inhibits the isotropic s-wave superconducting response leading the system to prefer order parameters of higher angular momenta. A quite general analysis of the interplay between on-site repulsion and neighbour and next-neighbour attraction has shown s-wave to d-wave crossover depending on the microscopic parameters of a model BCS Hamiltonian [16].

The purpose of the present paper is to study how the d-wave superconducting response resulting from a strongly momentum dependent total interaction, is affected by the inclusion of nonadiabatic vertex corrections. In particular, we intend to clarify whether the complex momentum-frequency structure of the nonadiabatic contributions could sustain an underlying d-wave symmetry of the order parameter.

In the next section we introduce the model and the corresponding ME equations for s- and d wave symmetries of the gap. In Section 3 we generalize the ME equations to include the nonadiabatic terms for each symmetry channel and calculate the corresponding critical temperatures. We find that the theory of nonadiabatic superconductivity can lead to d-wave even for phonons in a broad parameter range which depends on the degree of electronic correlation.

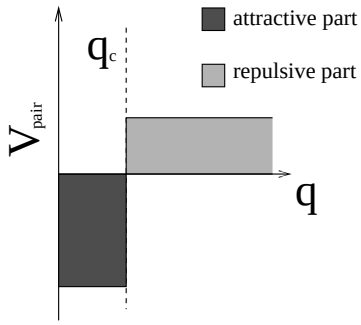

Fig. 1. Sketch of the total (el-ph + Coulomb) interaction in momentum space.

2 The model

In this section we introduce a simple model interaction suitable for our investigation beyond Migdal's limit and capable of providing for s- or d-wave symmetries of the order parameter. Let us consider the anomalous self-energy at the critical temperature

$$\Sigma_{\rm S}(k) = \sum_{k'} V_{\rm pair}(k-k')G(k')G(-k')\Sigma_{\rm S}(k'), \qquad (1)$$

where $G(k')$ is the fermion dressed propagator:

$$G(k') = \frac{1}{{\rm i}\omega_m - \epsilon_{\mathbf{k}'} - \Sigma_{\rm N}(k')} \qquad (2)$$

and $\Sigma_{\rm N}$ is the normal self-energy. We use the compact notation $k \equiv (\mathbf{k}, \omega_n)$, $k' \equiv (\mathbf{k}', \omega_m)$ and $\sum_{k'} \equiv -T_c \sum_m \sum_{\mathbf{k}'}$ where ω_n, ω_m are fermionic Matsubara frequencies and $\mathbf{k}$, $\mathbf{k}'$ are electronic momenta (from now on, all momenta are two-dimensional vectors lying on the copper-oxygen plane).

To define the model interaction $V_{\rm pair}(k-k')$ we have made use of a number of informations gathered from previous studies. First, in order to obtain order parameters with higher angular momenta than s-wave, it is sufficient to consider a pair interaction made of a repulsive part at short distances and an attractive one at higher distances (Fig. 1). In momentum space, this interaction corresponds to an attractive coupling for small $\mathbf{q}$ and a repulsive one for large $\mathbf{q}$, where $\mathbf{q} = \mathbf{k} - \mathbf{k}'$ is the momentum transfer.

Let us now try to interpret this strong momentum modulation in terms of e-ph and electron-electron interactions. In strongly correlated systems, the e-ph interaction acquires an important momentum dependence in such a way that for large values of the momentum transfer $\mathbf{q}$ the e-ph interaction is suppressed, whereas for small values of $\mathbf{q}$ it is enhanced [17]. A physical picture to justify this momentum modulation is the following [18]. In many-electrons systems a single charge carrier is surrounded by its own correlation hole of size ξ which can be much larger than the lattice parameter a in the strongly correlated regime. This implies that one electron interacts with molecular vibrations of wavelength of order ξ or larger, leading to an effective upper cut-off $q_c \simeq \xi^{-1}$ in the momenta space. Thus we have a non zero electron-phonon

interaction when $|\mathbf{q}| < q_c$. The cut-off momentum q_c can also be regarded as a measure of the correlation in the system: $aq_c \ll 1$ in strongly correlated systems while $aq_c \simeq 1$ in the case of free electrons.

From the above considerations, the attractive part at small $\mathbf{q}$ of our model pairing interaction finds a natural interpretation in the e-ph coupling modified by the strong electron correlations. We introduce therefore the following simple form for the e-ph part of the pairing interaction:

$$V(k-k') = |g(\mathbf{k}-\mathbf{k}')|^2 D(\omega_n - \omega_m) \equiv g^2 \left[\frac{\pi k_F}{q_c}\right] \theta(q_c - |\mathbf{k}-\mathbf{k}'|) D(\omega_n - \omega_m), \tag{3}$$

where

$$D(\omega_n - \omega_m) = \frac{-\omega_0^2}{(\omega_n - \omega_m)^2 + \omega_0^2}, \tag{4}$$

is the phonon propagator for which we have adopted a simple Einstein spectrum with frequency ω_0. In equation (3), θ is the Heaviside step function and the prefactor $(\pi k_F/q_c)$ has been introduced in order to assure that the momentum average of $|g(\mathbf{k}-\mathbf{k}')|^2$ becomes g^2 for relatively small values of the cut-off q_c regardless of the particular symmetry of the order parameter. In this way the comparison between *s*- and *d*-wave solutions, especially in the nonadiabatic case treated in the next section, is more transparent.

Having defined the nature of the attractive part of the total pairing interaction $V_{\rm pair}(k-k')$, we offer now a possible interpretation for the remaining repulsive part acting at large $\mathbf{q}$. This repulsion is given by the residual e-e interaction and its momentum dependence can be obtained, in analogy with the renormalization of the e-ph interaction, by using the above picture of correlation holes. In this picture, the residual e-e interaction should ensure that charge fluctuations with wavelength less than ξ are unfavourable. This can be modelled by requiring that in momentum space the residual interaction is repulsive for $|\mathbf{k}-\mathbf{k}'| > q_c$ and, by using again the theta-function for later convenience, we introduce therefore the following residual repulsion:

$$U(\mathbf{k}-\mathbf{k}') = U\left[\frac{\pi k_F}{q_c}\right] \theta(|\mathbf{k}-\mathbf{k}'| - q_c). \tag{5}$$

In the above expression, $U > 0$ and the factor $\pi k_F/q_c$ has been introduced for the same reason as in equation (3). Note that, in principle, q_c depends on U, however here we shall treat two quantities independently on each other by keeping in mind that small values of q_c correspond roughly to large values of U. An additional simplification of the following calculations is achieved by expressing the off-diagonal self-energy (1) in terms of a suitable pseudopotential U^* rather then U. It is then opportune to formally replace equation (5) by

$$U^*(k-k') = U^*\left[\frac{\pi k_F}{q_c}\right] \theta(|\mathbf{k}-\mathbf{k}'| - q_c) \frac{\omega_0^2}{(\omega_n - \omega_m)^2 + \omega_0^2}, \tag{6}$$

where U^* represents the dynamically screened Coulomb repulsion and the last factor is a cut-off over the Matsubara frequencies which has been chosen to have the same functional form of the phonon propagator for convenience.

By summarizing the above results, in the off-diagonal self-energy Σ_S, equation (1), the total pairing interaction $V_{\rm pair}(k-k')$ is given by:

$$V_{\rm pair}(k-k') = V(k-k') + U^*(k-k'), \tag{7}$$

where $V(k-k')$ and $U^*(k-k')$ are given by equations (3, 6), respectively. Finally, the normal state self-energy Σ_N entering (2) is given by

$$\Sigma_N(\omega_n) = \sum_{k'} V(k-k') G(k'), \tag{8}$$

where the electron-electron interaction has been absorbed in a shift of the chemical potential.

In what follows we assume the Fermi surface to be a circle in the momenta space; thus the electronic energy $\epsilon_{\mathbf{k}}$ depends only on $|\mathbf{k}|$. Moreover, we approximate equations (3) and (6) by keeping $|\mathbf{k}| = |\mathbf{k}'| = k_F$ so that, for example, $\mathbf{k} = k_F(\cos\phi, \sin\phi)$. In this way both Σ_S and Σ_N depend on the momentum $\mathbf{k}$ only *via* the angle ϕ. At this point it is convenient to transform the momentum integrations appearing in Σ_S and Σ_N into energy integrations as follows:

$$\sum_{\mathbf{k}} \to \int \frac{d\phi}{2\pi} \int d\epsilon N(\epsilon) \tag{9}$$

where $N(\epsilon)$ is the density of states for the electrons. We make the approximation of constant value for $N(\epsilon) = N_0$ and finite bandwidth E such that the energy is defined in the interval $-E/2 \le \epsilon \le E/2$. The chemical potential is $\mu = 0$, so that we refer to the half-filled situations ($E_F = E/2$).

On performing the integration over the energy, the anomalous self-energy Σ_S reduces to:

$$\Sigma_S(\phi, \omega_n) = N_0 \pi T_c \sum_{\omega_m} \int \frac{d\phi'}{2\pi} \left[|g(\cos\theta)|^2 - U^*(\cos\theta)\right] \times D(\omega_n - \omega_m) \frac{\Sigma_S(\phi', \omega_m)}{|\omega_m| Z(\phi', \omega_m)} \frac{2}{\pi} \arctan\left[\frac{E/2}{|\omega_m| Z(\phi', \omega_m)}\right], \tag{10}$$

$$Z(\phi, \omega_n) = 1 - N_0 \frac{\pi T_c}{\omega_n} \sum_{\omega_m} \int \frac{d\phi'}{2\pi} |g(\cos\theta)|^2 D(\omega_n - \omega_m) \times \frac{\omega_m}{|\omega_m|} \frac{2}{\pi} \arctan\left[\frac{E/2}{|\omega_m| Z(\phi', \omega_m)}\right], \tag{11}$$

where $\Sigma_N(\phi, \omega_n) = i\omega_n[1 - Z(\phi, \omega_n)]$ and $\theta = \phi - \phi'$. The wave function renormalization $Z(\phi, \omega_n)$ actually does not depend on ϕ and reduces to:

$$Z(\omega_n) = 1 - N_0 \langle g^2 \rangle_0 \frac{\pi T_c}{\omega_n} \sum_{\omega_m} D(\omega_n - \omega_m) \frac{\omega_m}{|\omega_m|} \times \frac{2}{\pi} \arctan\left[\frac{E/2}{|\omega_m| Z(\omega_m)}\right], \tag{12}$$

where $\langle g^2\rangle_0 = \int_{-\pi}^{\pi} \mathrm{d}\theta |g(\cos\theta)|^2/(2\pi)$. Let us expand the off-diagonal self-energy (10) as follows:

$$\Sigma_{\rm S}(\phi,\omega_n) = \sum_{l=-\infty}^{+\infty} \Sigma_{\rm S}^{(l)}(\omega_n) Y_l(\phi) \ , \tag{13}$$

where $Y_l(\phi) = \mathrm{e}^{\mathrm{i}l\phi}/\sqrt{2\pi}$ are eigenfunctions of the operator $L = -\mathrm{i}\mathrm{d}/\mathrm{d}\phi$. By requiring $\Sigma_{\rm S}(\phi,\omega_n)$ be real and invariant under $\phi \to \phi \pm \pi$ (singlet pairing) the above expansion reduces to:

$$\Sigma_{\rm S}(\phi,\omega_n) = \frac{\Sigma_{\rm S}^{(0)}(\omega_n)}{\sqrt{2\pi}} + \sqrt{\frac{2}{\pi}}\Sigma_{\rm S}^{(2)}(\omega_n)\cos(2\phi) + \cdots \ , \tag{14}$$

where we have singled out the s-wave and d-wave components since in the following we consider only these symmetries. By multiplying both sides of (10) by $Y_{l'}^*(\phi)$ and integrating over ϕ, it is straightforward to show that the equations for different values of the index l are decoupled and that $\Sigma_{\rm S}^{(l)}(\omega_n)$ reduces to:

$$\Sigma_S^{(l)}(\omega_n) = -\ N_0 \left[\langle g^2\rangle_l - \langle U^*\rangle_l\right] \pi T_{\rm c} \sum_{\omega_m} D(\omega_n - \omega_m) \times \frac{\Sigma_S^{(l)}(\omega_m)}{|\omega_m| Z(\omega_m)} \frac{2}{\pi} \arctan\left[\frac{E/2}{|\omega_m| Z(\omega_m)}\right], \tag{15}$$

where

$$\langle g^2\rangle_l = \frac{1}{2\pi}\int_{-\pi}^{\pi} \mathrm{d}\theta \ |g(\cos\theta)|^2 \mathrm{e}^{-\mathrm{i}l\theta} \tag{16}$$

$$\langle U^*\rangle_l = \frac{1}{2\pi}\int_{-\pi}^{\pi} \mathrm{d}\theta \ U^*(\cos\theta) \mathrm{e}^{-\mathrm{i}l\theta}. \tag{17}$$

Finally, by introducing the coupling constants $\lambda_l = N_0\langle g^2\rangle_l$, $\mu_l^* = N_0\langle U^*\rangle_l$, and by setting $\Delta_l = \Sigma_{\rm S}^{(l)}/Z$, the Eliashberg equations assume the following more familiar form:

$$Z(\omega_n) = 1 \ -\lambda_0 \frac{\pi T_{\rm c}}{\omega_n} \sum_{\omega_m} D(\omega_n - \omega_m) \frac{\omega_m}{|\omega_m|} \times \frac{2}{\pi} \arctan\left[\frac{E/2}{|\omega_m| Z(\omega_m)}\right], \tag{18}$$

$$Z(\omega_n)\Delta_l(\omega_n) = -\ (\lambda_l - \mu_l^*)\, \pi T_{\rm c} \sum_{\omega_m} D(\omega_n - \omega_m) \frac{\Delta_l(\omega_m)}{|\omega_m|} \times \frac{2}{\pi} \arctan\left[\frac{E/2}{|\omega_m| Z(\omega_m)}\right]. \tag{19}$$

For $l = 0$ and $l = 2$, equations (18, 19) are Migdal-Eliashberg equations for s-wave and d-wave symmetry channels, respectively. The explicit expressions of the constants λ_l and μ_l^* follow from the models we adopted for the electron-phonon and electron-electron interactions. For $l = 0$ (s-wave) they reduce to:

$$\lambda_0 = \lambda \left[\frac{\pi k_{\rm F}}{q_{\rm c}}\right] \langle \theta(q_{\rm c} - |\mathbf{k} - \mathbf{k}'|)\rangle_{l=0} = \lambda \frac{\arcsin Q_{\rm c}}{Q_{\rm c}}, \tag{20}$$

$$\mu_0^* = \mu^* \left[\frac{\pi k_{\rm F}}{q_{\rm c}}\right] \langle \theta(|\mathbf{k} - \mathbf{k}'| - q_{\rm c})\rangle_{l=0} = \mu^* \left(\frac{\pi}{2Q_{\rm c}} - \frac{\arcsin Q_{\rm c}}{Q_{\rm c}}\right), \tag{21}$$

while for $l = 2$ (d-wave):

$$\lambda_2 = \lambda \left[\frac{\pi k_{\rm F}}{q_{\rm c}}\right] \langle \theta(q_{\rm c} - |\mathbf{k} - \mathbf{k}'|)\rangle_{l=2} = \lambda(1 - 2Q_{\rm c}^2)\sqrt{1 - Q_{\rm c}^2}, \tag{22}$$

$$\mu_2^* = \mu^* \left[\frac{\pi k_{\rm F}}{q_{\rm c}}\right] \langle \theta(|\mathbf{k} - \mathbf{k}'| - q_{\rm c})\rangle_{l=2} = -\mu^*(1 - 2Q_{\rm c}^2)\sqrt{1 - Q_{\rm c}^2}, \tag{23}$$

where $\lambda = N_0 g^2$, $\mu^* = N_0 U^*$ and $Q_{\rm c} = q_{\rm c}/2k_{\rm F}$. Before we generalize the above expressions to include the nonadiabatic vertex corrections, it is useful to briefly examine qualitatively how the the magnitude of the cut-off parameter $Q_{\rm c}$ affects the gap symmetry. The total interaction in the gap equation (19) is weighted by $\lambda_l - \mu_l^*$. For the s-wave channel it reduces to:

$$\lambda_0 - \mu_0^* = (\lambda + \mu^*)\frac{\arcsin Q_{\rm c}}{Q_{\rm c}} - \frac{\pi}{2Q_{\rm c}}\mu^*, \tag{24}$$

while for the d-wave case $l = 2$ it becomes:

$$\lambda_2 - \mu_2^* = (\lambda + \mu^*)(1 - 2Q_{\rm c}^2)\sqrt{1 - Q_{\rm c}^2}. \tag{25}$$

When $Q_{\rm c} = 1$ (that is $q_{\rm c} = 2k_{\rm F}$) the repulsive interaction (6) vanishes and the e-ph coupling (3) becomes structureless. In this limit we expect the s-wave solution to dominate over the d-wave one. In fact, from (24, 25), $\lambda_0 - \mu_0^* = \lambda$ and $\lambda_2 - \mu_2^* = 0$. By lowering $Q_{\rm c}$, the total interaction acquires a momentum dependence, however $\lambda_2 - \mu_2^*$ remains negative as long as $1/\sqrt{2} < Q_{\rm c} < 1$. In this range therefore there is not d-wave solution. By further lowering of the cut-off parameter, the d-wave symmetry begins to compete with the s-wave one and for $Q_{\rm c} \ll 1$ $\lambda_2 - \mu_2^* \simeq \lambda + \mu^*$ while $\lambda_0 - \mu_0^* \simeq -\pi\mu^*/2Q_{\rm c}$ signalling that the d-wave symmetry overcomes the s-wave ones.

In previous studies, we have shown that the nonadiabatic corrections lead to an enhancement of the critical temperature for small values of $Q_{\rm c}$ in the s-wave channel. However in the present model, small values of $Q_{\rm c}$ lead to a solution with d-wave symmetry and the question we face in the following sections is whether also in this symmetry the nonadiabatic corrections provide for an amplification of $T_{\rm c}$.

3 Non adiabatic vertex corrections

In this section we introduce the first corrections arising from the breakdown of Migdal's theorem in the equations for the normal and anomalous self-energies. By following reference [7], the first nonadiabatic corrections to the e-ph

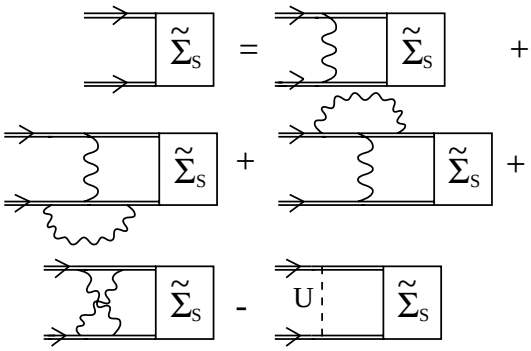

Fig. 2. Self-consistent gap equation including the first corrections beyond Migdal's theorem

interaction affect the normal state self-energy (8) in the following way:

$$\widetilde{\Sigma}_{\rm N}(k) = \sum_{k'} \widetilde{V}_{\rm N}(k,k')G(k'), \tag{26}$$

$$\widetilde{V}_{\rm N}(k,k') = V(k-k') \times \left[1 + \sum_{q} V(k-q)G(q-k+k')G(q)\right], \tag{27}$$

where the last term in the square bracket of equation (27) defines the vertex function. The off-diagonal self-energy in the nonadiabatic regime is instead modified as follows:

$$\widetilde{\Sigma}_{\rm S}(k) = \sum_{k'} \left[\widetilde{V}_{\rm S}(k,k') - U^*(k-k')\right] \times G(k')G(-k')\widetilde{\Sigma}_{\rm S}(k'), \tag{28}$$

$$\widetilde{V}_{\rm S}(k,k') = V(k-k')\left[1 + \sum_{q} V(k-q)G(q)G(q-k+k') + \sum_{q} V(k-q)G(-q)G(-q+k-k')\right] + \sum_{q} V(k-q)V(q-k')G(q)G(q-k-k'), \tag{29}$$

where $q \equiv (\mathbf{q}, \omega_l)$ and $U^*(k-k')$ is given by equation (6). The second and the third terms within the square brackets in equation (29) correspond to the first order vertex corrections, while the last term corresponds to the cross scattering. These non adiabatic terms are shown in Figure 2 in which we are only include these terms that give a finite contribution for $T = T_{\rm c}$.

In the vertex corrections there is simple one-phonon interaction, while in the cross term the sum refers to the product of both phonon propagators. This product of phonon propagators can be approximated as [7]:

$$\frac{\omega_0^2}{(\omega_n-\omega_l)^2+\omega_0^2}\frac{\omega_0^2}{(\omega_l-\omega_m)^2+\omega_0^2} \simeq \frac{\omega_0^2}{(\omega_n-\omega_m)^2+\omega_0^2}\frac{\omega_0^2}{(\omega_n-\omega_l)^2+\omega_0^2}\,. \tag{30}$$

For the momentum dependence in the electron-phonon coupling we can approximate

$$|g(\mathbf{k}-\mathbf{q})|^2|g(\mathbf{q}-\mathbf{k}')|^2 \simeq |g(\mathbf{k}-\mathbf{k}')|^2|g(\mathbf{k}-\mathbf{q})|^2. \tag{31}$$

This approximation is valid for relatively small values of the cut-off $q_{\rm c}$. Therefore the last term in equation (29) reduces to:

$$\sum_{q} V(k-q)V(q-k')G(q)G(q-k-k') \simeq V(k-k')\sum_{q} V(k-q)G(q)G(q-k-k')\,. \tag{32}$$

At this point it is useful to introduce a compact notation for the vertex and cross functions:

$$P_{\rm V}(k,k') \equiv \frac{1}{\lambda}\sum_{q} V(k-q)G(q)G(q-k+k')\,, \tag{33}$$

$$P_{\rm C}(k,k') \equiv \frac{1}{\lambda}\sum_{q} V(k-q)G(q)G(q-k-k')\,. \tag{34}$$

Thus equations (27, 29) may be written in a simpler way as follows:

$$\widetilde{V}_{\rm N}(k,k') = V(k-k')\left[1+\lambda P_{\rm V}(k,k')\right], \tag{35}$$

$$\widetilde{V}_{\rm S}(k,k') = V(k-k')\left[1+2\lambda P_{\rm V}(k,k') + \lambda P_{\rm C}(k,k')\right]. \tag{36}$$

In equation (28), the momentum dependence of $\widetilde{\Sigma}_{\rm S}(k)$ is transformed as in equation (13) and the interaction term $\widetilde{V}_{\rm S}(k,k')$ is replaced by its angular weighted average:

$$\langle\widetilde{V}_{\rm S}(k,k')\rangle_l = \frac{1}{2\pi}\int_{-\pi}^{\pi} {\rm d}\theta\ \widetilde{V}_{\rm S}(\cos\theta){\rm e}^{-{\rm i}l\theta}\,, \tag{37}$$

which in terms of averaged vertex and cross corrections is expressed as:

$$\langle\widetilde{V}_{\rm S}(k,k')\rangle_l = \langle V(k-k')\rangle_l + 2\lambda\langle V(k-k')P_{\rm V}(k,k')\rangle_l + \lambda\langle V(k-k')P_{\rm C}(k,k')\rangle_l. \tag{38}$$

The first term in the r.h.s. contains only the e-ph interaction and the phonon propagator and it is simply given by:

$$\langle V(k-k')\rangle_l = g^2 D(\omega_n-\omega_m)\left[\frac{\pi k_{\rm F}}{q_{\rm c}}\right]\langle\theta(q_{\rm c}-|\mathbf{k}-\mathbf{k}'|)\rangle_l = \frac{\lambda_l}{N_0}D(\omega_n-\omega_m), \tag{39}$$

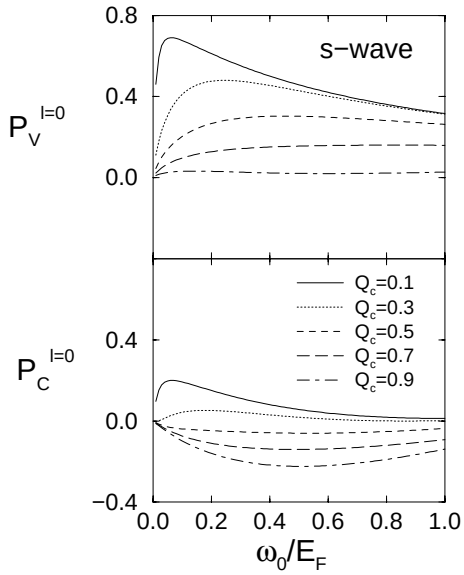

Fig. 3. Behavior of the vertex (top panel) and cross (bottom panel) functions in the s-wave channel for different values of the cut-off parameter Q_c. The case shown refers to the parameters $\omega_n = 0$, $\omega_m = \omega_0$.

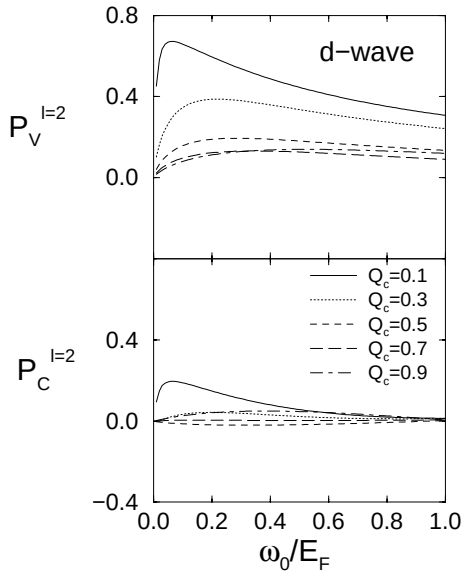

Fig. 4. Behavior of the vertex (top panel) and cross (bottom panel) functions in the d-wave channel for different values of the cut-off parameter Q_c. The case shown refers to the parameters $\omega_n = 0$, $\omega_m = \omega_0$.

where λ_l for $l = 0$ and $l = 2$ is given in equations (20, 22), respectively. The second and third terms of (38) correspond instead to the momentum averages of the nonadiabatic corrections

$$\begin{aligned}\langle V(k-k')P_{\rm V}(k,k')\rangle_l &= g^2 D(\omega_n-\omega_m)P^l_{\rm V}(\omega_n,\omega_m,q_{\rm c}),\\ \langle V(k-k')P_{\rm C}(k,k')\rangle_l &= g^2 D(\omega_n-\omega_m)P^l_{\rm C}(\omega_n,\omega_m,q_{\rm c}),\end{aligned} \tag{40}$$

where

$$\begin{aligned}P^l_{\rm V}(\omega_n,\omega_m,q_{\rm c}) &= \left[\frac{\pi k_{\rm F}}{q_{\rm c}}\right]\langle\theta(q_{\rm c}-|\mathbf{k}-\mathbf{k}'|)P_{\rm V}(k,k')\rangle_l\\ P^l_{\rm C}(\omega_n,\omega_m,q_{\rm c}) &= \left[\frac{\pi k_{\rm F}}{q_{\rm c}}\right]\langle\theta(q_{\rm c}-|\mathbf{k}-\mathbf{k}'|)P_{\rm C}(k,k')\rangle_l.\end{aligned} \tag{41}$$

Analytic expressions of the vertex and cross functions together with their averages $P^l_{\rm V}$ and $P^l_{\rm C}$ for $l = 0$ and $l = 2$ are reported in Appendix and the results are shown in Figures 3 and 4 as function of the adiabatic parameter $\omega_0/E_{\rm F}$ and for different values of dimensionless cut-off $Q_{\rm c} = q_{\rm c}/2k_{\rm F}$. All the curves have been obtained by setting $\omega_n = 0$ and $\omega_m = \omega_0$ so that the exchanged frequency equals ω_0. The behaviors, particularly at small $Q_{\rm c}$, of $P^l_{\rm V}$ and $P^l_{\rm C}$ are essentially independent of the particular symmetry. In fact for both $l = 0$ (s-wave) and $l = 2$ (d-wave) the nonadiabatic corrections are positive leading to an enhancement of the total e-ph interaction. We expect therefore that, as for the s-wave case [6,7], also for the d-wave symmetry the vertex and cross corrections tend to amplify $T_{\rm c}$ when $Q_{\rm c}$ is sufficiently small.

To verify this point, we can write down the nonadiabatic Eliashberg equations for different symmetry channels. As in the previous section, the normal state self-energy (26) is averaged over the Fermi surface and, according to (35), $\widetilde{V}_{\rm N}(k,k')$ reduces to:

$$\begin{aligned}\widetilde{V}_{\rm N}(k,k') &\to \langle\widetilde{V}_{\rm N}(k,k')\rangle_{l=0}\\ &= \frac{D(\omega_n-\omega_m)}{N_0}\left[\lambda_0+\lambda^2 P^{l=0}_{\rm V}(\omega_n,\omega_m,q_{\rm c})\right],\end{aligned} \tag{42}$$

and $Z(\omega_n) = 1 - \widetilde{\Sigma}^{(0)}_{\rm N}(\omega_n)/{\rm i}\omega_n$ becomes:

$$\begin{aligned}Z(\omega_n) = 1 &- \frac{\pi T_{\rm c}}{\omega_n}\sum_m\left[\lambda_0+\lambda^2 P^{l=0}_{\rm V}(\omega_n,\omega_m,q_{\rm c})\right]\\ &\times D(\omega_n-\omega_m)\frac{\omega_m}{|\omega_m|}\frac{2}{\pi}\arctan\left[\frac{E/2}{|\omega_m|Z(\omega_m)}\right].\end{aligned} \tag{43}$$

Finally, the gap function for different symmetry channels is:

$$\begin{aligned}Z(\omega_n)\Delta_l(\omega_n) = -\pi T_{\rm c}\sum_{\omega_m}&[\lambda_l + 2\lambda^2 P^l_{\rm V}(\omega_n,\omega_m,q_{\rm c})\\ &+\lambda^2 P^l_{\rm C}(\omega_n,\omega_m,q_{\rm c}) - \mu^*_l]D(\omega_n-\omega_m)\frac{\Delta_l(\omega_m)}{|\omega_m|}\\ &\times\frac{2}{\pi}\arctan\left[\frac{E/2}{|\omega_m|Z(\omega_m)}\right]\end{aligned} \tag{44}$$

where μ^*_l is given by equations (21, 23) and $l = 0, 2$.

To establish the range of $Q_{\rm c}$ values in which the d-wave symmetry is more stable than s-wave one and to quantify the effect of nonadiabaticity, we solve numerically the generalized Eliashberg equations (43, 44) for $l = 0$ and $l = 2$. To find $T_{\rm c}$, we follow the maximum eigenvalue method

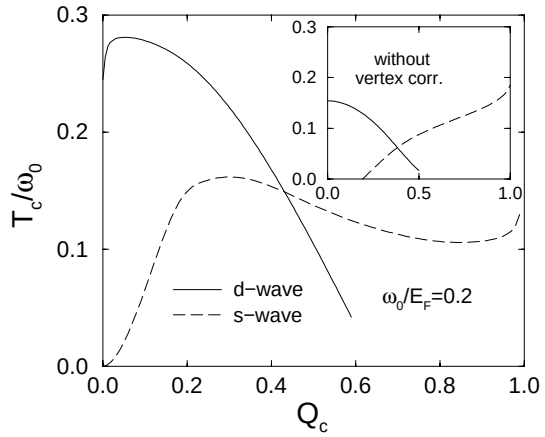

Fig. 5. Behaviour of the critical temperature T_c as function of Q_c in the *s*- and *d*-wave symmetry channels. The case shown refers to the parameters $\lambda = 1$ and $\mu^* = 0.1$. In the inset it is shown the case without nonadiabatic corrections.

described for example in [7]. The resulting values of T_c as a function of Q_c are shown in Figure 5 for the *d*- and *s*-wave symmetries. In the inset we show the critical temperature calculated without the vertex and cross corrections, *i.e.*, for the ME equations (18, 19). To display the crossover between the *d*- and the *s*-wave symmetries more clearly, we show the results for $\lambda = 1$ and $\mu^* = 0.1$. When $\mu^* \simeq \lambda$ in fact the *s*-wave symmetry is suppressed by the strong repulsive interaction.

By reducing Q_c, the *s*-wave solution (dashed lines) decreases monotonically when the vertex and cross corrections are not included (inset) while for the nonadiabatic case the corresponding T_c shows an upturn before falling to zero at $Q_c \to 0$. This latter feature is due to the nonadiabatic corrections which become more positive when Q_c is small. For lower values of Q_c, however, the pseudopotential is dominant and T_c falls rapidly to zero. Contrary to the isotropic case, the *d*-wave solutions (solid lines) lead to critical temperatures which increase when Q_c is lowered. Since, as discussed before, the vertex corrections have a similar behavior both in *d*- and in *s*-wave symmetries when Q_c is small, the critical temperature in the nonadiabatic case is enhanced compared to the solution without vertex and cross corrections.

It is finally interesting to compare the present results with the phenomenology of the superconducting copper-oxides, which show *d*-wave, and the fullerides, which instead show *s*-wave. In our perspective there are important differencies between the two materials. A relevant one is that the oxides have their largest values of T_c when the Fermi surface is strongly influenced by van Hove singularities. Then correlation effects can be estimated to be larger in the oxides and, finally, fullerides seem to have rotational disorder which would favour *s*-wave. Therefore, in principle, it could happen that in the oxides, going into the overdoped phase might lead to a crossover from *d*-wave to *s*-wave depending on the parameters.

4 Conclusions

In isotropic *s*-wave superconductors, the first nonadiabatic corrections to the e-ph interaction such as vertex and cross functions are strongly dependent on the momentum transfer $\mathbf{q}$. In particular, small values of $\mathbf{q}$ leads to positive nonadiabatic corrections inducing an enhancement of the critical temperature T_c [6,7]. Here, we have addressed the problem of the momentum dependence of the nonadiabatic corrections for a *d*-wave symmetry of the order parameter. By introducing a model interaction in which the e-ph interaction is dominant at small values of $\mathbf{q}$ and the residual repulsion of electronic origin is instead important at larger momentum transfers, we have shown that also when the solution has *d*-wave symmetry, the inclusion of nonadiabatic corrections enhances T_c compared to the case without corrections. Therefore in a strongly correlated system, for which the e-ph interaction is mainly of forward scattering, *d*-wave superconductivity driven by phonons can be sustained by the nonadiabatic corrections

Appendix A: Analytical calculation of vertex and cross functions

A.1 Vertex function

The evaluation of the vertex function given in equation (33) follows basically the same lines and approximations made in reference [7], the main difference being that here we refer to a two-dimensional system rather than a three-dimensional one. Making use of the linear model for the electronic dispersion and considering the limit of $T_c/\omega_0 \ll 1$, we obtain

$$P_{\rm V}(k,k') = \frac{\omega_0}{2\lambda}\sum_{\mathbf{q}} \frac{|g(\mathbf{k}-\mathbf{q})|^2}{\epsilon_{\mathbf{q}} - \epsilon_{\mathbf{q}-\mathbf{k}+\mathbf{k}'} - {\rm i}\omega_n + {\rm i}\omega_m} \times \left[-\frac{\theta(\epsilon_{\mathbf{q}})}{\epsilon_{\mathbf{q}} + \omega_0 - {\rm i}\omega_n} - \frac{\theta(-\epsilon_{\mathbf{q}})}{\epsilon_{\mathbf{q}} - \omega_0 - {\rm i}\omega_n} + \frac{\theta(\epsilon_{\mathbf{q}-\mathbf{k}+\mathbf{k}'})}{\epsilon_{\mathbf{q}-\mathbf{k}+\mathbf{k}'} + \omega_0 - {\rm i}\omega_m} + \frac{\theta(-\epsilon_{\mathbf{q}-\mathbf{k}+\mathbf{k}'})}{\epsilon_{\mathbf{q}-\mathbf{k}+\mathbf{k}'} - \omega_0 - {\rm i}\omega_m} \right]. \quad \text{(A.1)}$$

The main difficulty comes from $\epsilon_{\mathbf{q}-\mathbf{k}+\mathbf{k}'}$ which, within our model, is

$$\epsilon_{\mathbf{q}-\mathbf{k}+\mathbf{k}'} = v_{\rm F}[q^2 + k\prime^2 + k^2 - 2qk\cos\alpha + 2qk'\cos\beta - 2kk'\cos\theta]^{1/2} - \mu, \quad \text{(A.2)}$$

where α, β and θ are the angles between the directions of $(\mathbf{q},\mathbf{k})$, $(\mathbf{q},\mathbf{k}')$ and $(\mathbf{k},\mathbf{k}')$ respectively. In the limit of small q_c, the presence of θ-function in front of $P_{\rm V}$ (Eq. (41)) and inside of the integral leads to $|\mathbf{k}| \sim |\mathbf{k}'|$ and $|\mathbf{k}| \sim |\mathbf{q}|$. Therefore equation (A.2) can be rewritten as follows:

$$\epsilon_{\mathbf{q}-\mathbf{k}+\mathbf{k}'} \simeq \epsilon_{\mathbf{q}} + v_{\rm F}k_{\rm F}\left[1 - \cos\alpha + \cos\beta - \cos\theta\right], \quad \text{(A.3)}$$

where we have taken $|\mathbf{k}| \simeq k_{\rm F}$. We can relate the angle β to α and θ by means of relation $\beta = \theta - \alpha$. Therefore

equation (A.3) becomes:

$$\epsilon_{\mathbf{q}-\mathbf{k}+\mathbf{k}'} \simeq \epsilon_{\mathbf{q}} + v_{\mathrm{F}} k_{\mathrm{F}} \left[(1-\cos\alpha)(1-\cos\theta) + \sin\alpha\sin\theta\right]. \tag{A.4}$$

If $Q = |\mathbf{k}-\mathbf{k}'|/2k_{\mathrm{F}}$ then $\cos\theta = 1-2Q^2$ and $\sin\theta = 2Q\sqrt{1-Q^2}$:

$$\epsilon_{\mathbf{q}-\mathbf{k}+\mathbf{k}'} \simeq \epsilon_{\mathbf{q}} + EQ^2(1-\cos\alpha) + EQ\sqrt{1-Q^2}\sin\alpha\ . \tag{A.5}$$

Expanding $\cos\alpha$ and $\sin\alpha$ in powers of α and retaining only the lowest order term in α and Q we finally obtain:

$$\epsilon_{\mathbf{q}-\mathbf{k}+\mathbf{k}'} \simeq \epsilon_{\mathbf{q}} + EQ\alpha\ . \tag{A.6}$$

For small q_{c} we can replace

$$\begin{aligned}\theta(q_{\mathrm{c}} - |\mathbf{k}-\mathbf{q}|) &\simeq \theta(q_{\mathrm{c}} - k_{\mathrm{F}}\sqrt{2(1-\cos\alpha)}) \\ &\simeq \theta(2Q_{\mathrm{c}} - |\alpha|)\ .\end{aligned} \tag{A.7}$$

At this point it is convenient to transform the momentum integration into an energy integration:

$$\int \frac{\mathrm{d}^2 q}{(2\pi)^2} = N_0 \int_{-\pi}^{\pi} \frac{\mathrm{d}\alpha}{2\pi} \int_{-E/2}^{E/2} \mathrm{d}\epsilon \tag{A.8}$$

where we have used a constant DOS $N(\epsilon) = N_0$ in the range $-E/2 \le \epsilon \le E/2$. The integration over the energy ϵ and over the angle α can be performed analytically and the final expression of the vertex function in the limit of small Q_{c} is given by

$$\begin{aligned}P_{\mathrm{V}}(k,k') = \omega_0 B(\omega_n,\omega_m) + \frac{\omega_0}{2Q_{\mathrm{c}}}\frac{1}{EQ}\arctan\left(\frac{2Q_{\mathrm{c}}EQ}{|\omega_n-\omega_m|}\right) \\ \times \frac{A(\omega_n,\omega_m) - B(\omega_n,\omega_m)(\omega_n-\omega_m)^2}{|\omega_n-\omega_m|}\ ,\end{aligned} \tag{A.9}$$

where $Q = |\mathbf{k}-\mathbf{k}'|/2k_{\mathrm{F}}$, $Q_{\mathrm{c}} = q_{\mathrm{c}}/2k_{\mathrm{F}}$, and

$$\begin{aligned}A(\omega_n,\omega_m) = (\omega_n-\omega_m)\left[\arctan\left(\frac{\omega_n}{\omega_0}\right) - \arctan\left(\frac{\omega_m}{\omega_0}\right)\right. \\ \left. + \arctan\left(\frac{\omega_m}{\omega_0+E/2}\right) - \arctan\left(\frac{\omega_n}{\omega_0+E/2}\right)\right],\end{aligned} \tag{A.10}$$

$$B(\omega_n,\omega_m) = -(\omega_0+E/2)\frac{(\omega_0+E/2)^2 + 2\omega_m^2 - \omega_n\omega_m}{\left[(\omega_0+E/2)^2+\omega_m^2\right]^2}\ . \tag{A.11}$$

A.2 Cross function

The function $P_{\mathrm{C}}(k,k')$, given by equation (34), can be explicitly evaluated within the same scheme of calculation of the vertex function. In the limit of $T_{\mathrm{c}}/\omega_0 \ll 1$ we have:

$$\begin{aligned}P_{\mathrm{C}}(k,k') = \frac{\omega_0}{2\lambda}\sum_{\mathbf{q}}\frac{|g(\mathbf{k}-\mathbf{q})|^2}{\epsilon_{\mathbf{q}} - \epsilon_{\mathbf{q}-\mathbf{k}-\mathbf{k}'} - \mathrm{i}\omega_n - \mathrm{i}\omega_m} \\ \times\left[-\frac{\theta(\epsilon_{\mathbf{q}})}{\epsilon_{\mathbf{q}}+\omega_0-\mathrm{i}\omega_n} - \frac{\theta(-\epsilon_{\mathbf{q}})}{\epsilon_{\mathbf{q}}-\omega_0-\mathrm{i}\omega_n}\right. \\ \left. + \frac{\theta(\epsilon_{\mathbf{q}-\mathbf{k}-\mathbf{k}'})}{\epsilon_{\mathbf{q}-\mathbf{k}-\mathbf{k}'}+\omega_0+\mathrm{i}\omega_m} + \frac{\theta(-\epsilon_{\mathbf{q}-\mathbf{k}-\mathbf{k}'})}{\epsilon_{\mathbf{q}-\mathbf{k}-\mathbf{k}'}-\omega_0+\mathrm{i}\omega_m}\right].\end{aligned} \tag{A.12}$$

The electron energy $\epsilon_{\mathbf{q}-\mathbf{k}-\mathbf{k}'}$ can be approximated for $q_{\mathrm{c}} \ll 2k_{\mathrm{F}}$ as follows:

$$\begin{aligned}\epsilon_{\mathbf{q}-\mathbf{k}-\mathbf{k}'} &= v_{\mathrm{F}}[q^2 + k\prime^2 + k^2 - 2qk\cos\alpha - 2qk'\cos\beta \\ &\quad + 2kk'\cos\theta]^{1/2} - \mu \\ &\simeq \epsilon_{\mathbf{q}} + E(1-Q^2)\frac{\alpha^2}{2} - EQ\sqrt{1-Q^2}\alpha.\end{aligned} \tag{A.13}$$

The integrations over the energy and the angle are elementary, the final expression of the cross function is however quite complicated:

$$\begin{aligned}P_{\mathrm{C}}(k,k') = \omega_0 B(\omega_n,-\omega_m) - \frac{\omega_0}{2Q_{\mathrm{c}}}\frac{1}{E\sqrt{1-Q^2}\rho(k,k')} \\ \times\{\cos[\eta(k,k')]C(k,k') + \sin[\eta(k,k')]D(k,k')\} \\ \times\frac{A(\omega_n,-\omega_m) - B(\omega_n,-\omega_m)(\omega_n+\omega_m)^2}{|\omega_n+\omega_m|},\end{aligned} \tag{A.14}$$

where the functions A and B are the same of equations (A.10, A.11) with $\omega_m \to -\omega_m$. The function C, D, η, ρ are given by

$$\rho(k,k') = \left[Q^4 + \left(2\frac{\omega_n+\omega_m}{E}\right)^2\right]^{1/4}\ , \tag{A.15}$$

$$\eta(k,k') = -\frac{1}{2}\arctan\left(\frac{2|\omega_n+\omega_m|}{EQ^2}\right)\ , \tag{A.16}$$

$$\begin{aligned}C(k,k') = b(k,k')^2\left\{\arctan\left[\frac{a_+(k,k')}{b(k,k')}\right]\right. \\ +\arctan\left[\frac{a_-(k,k')}{b(k,k')}\right] + \arctan\left[\frac{2Q_{\mathrm{c}} - a_+(k,k')}{b(k,k')}\right] \\ \left. + \arctan\left[\frac{2Q_{\mathrm{c}} - a_-(k,k')}{b(k,k')}\right]\right\},\end{aligned} \tag{A.17}$$

$$\begin{aligned}D(k,k') = \frac{1}{2}\ln\left\{\frac{[2Q_{\mathrm{c}} - a_+(k,k')]^2 + b(k,k')^2}{[2Q_{\mathrm{c}} - a_-(k,k')]^2 + b(k,k')^2}\right. \\ \left.\times\frac{a_-(k,k')^2 + b(k,k')^2}{a_+(k,k')^2 + b(k,k')^2}\right\}\ ,\end{aligned} \tag{A.18}$$

$$a_\pm(k,k') = \frac{Q \pm \rho(k,k')\cos[\eta(k,k')]}{\sqrt{1-Q^2}}\ , \tag{A.19}$$

$$b(k,k') = \frac{\rho(k,k')}{\sqrt{1-Q^2}}\sin[\eta(k,k')]\ . \tag{A.20}$$

A.3 s- and d-wave averages

In what follows we report the final expressions of the *s*-wave and *d*-wave averages of the vertex and cross functions defined in equation (41) for $l = 0$ (*s*-wave) and $l = 2$ (*d*-wave), where $P_{\rm V}$ and $P_{\rm C}$ are given by equations (A.9, A.14), respectively.

$$P_{\rm V}^{l=0}(\omega_n,\omega_m;q_{\rm c}) = \frac{A(\omega_n,\omega_m) - B(\omega_n,\omega_m)(\omega_n-\omega_m)^2}{|\omega_n-\omega_m|} \times \frac{\omega_0}{2EQ_c^2}F_1(\omega_n,\omega_m,Q_{\rm c}) + B(\omega_n,\omega_m)\frac{\arcsin Q_{\rm c}}{Q_{\rm c}} \quad \text{(A.21)}$$

$$P_{\rm C}^{l=0}(\omega_n,\omega_m;q_{\rm c}) = -\frac{A(\omega_n,-\omega_m) - B(\omega_n,-\omega_m)(\omega_n+\omega_m)^2}{|\omega_n+\omega_m|} \times \frac{\omega_0}{2EQ_c^2}F_2(\omega_n,\omega_m,Q_{\rm c}) + B(\omega_n,-\omega_m)\frac{\arcsin Q_{\rm c}}{Q_{\rm c}} \quad \text{(A.22)}$$

$$P_{rmV}^{l=2}(\omega_n,\omega_m;q_{\rm c}) = \frac{A(\omega_n,\omega_m) - B(\omega_n,\omega_m)(\omega_n-\omega_m)^2}{|\omega_n-\omega_m|} \times \frac{\omega_0}{2EQ_c^2}F_3(\omega_n,\omega_m,Q_{\rm c}) + B(\omega_n,\omega_m)(1-2Q_c^2)\sqrt{1-Q_c^2} \quad \text{(A.23)}$$

$$P_{\rm C}^{l=2}(\omega_n,\omega_m;q_{\rm c}) = -\frac{A(\omega_n,-\omega_m) - B(\omega_n,-\omega_m)(\omega_n+\omega_m)^2}{|\omega_n+\omega_m|}\frac{\omega_0}{2EQ_c^2} \times F_4(\omega_n,\omega_m,Q_{\rm c}) + B(\omega_n,-\omega_m)(1-2Q_c^2)\sqrt{1-Q_c^2} \quad \text{(A.24)}$$

where

$$F_1(\omega_n,\omega_m,Q_{\rm c}) = \int_0^{Q_{\rm c}} \frac{{\rm d}Q}{Q\sqrt{1-Q^2}} \arctan\left(\frac{2EQ_{\rm c}Q}{|\omega_n+\omega_m|}\right), \quad \text{(A.25)}$$

$$F_2(\omega_n,\omega_m,Q_{\rm c}) = \int_0^{Q_{\rm c}} \frac{{\rm d}Q}{Q}\left(\frac{1}{1-Q^2}\right)\frac{1}{\rho(k,k')} \times \{C(k,k')\cos[\eta(k,k')] - D(k,k')\sin[\eta(k,k')]\} \quad \text{(A.26)}$$

$$F_3(\omega_n,\omega_m,Q_{\rm c}) = \int_0^{Q_{\rm c}} \frac{{\rm d}Q}{Q}\left(\frac{1+8Q^4-8Q^2}{\sqrt{1-Q^2}}\right) \times \arctan\left(\frac{2EQ_{\rm c}Q}{|\omega_n+\omega_m|}\right), \quad \text{(A.27)}$$

$$F_4(\omega_n,\omega_m,Q_{\rm c}) = \int_0^{Q_{\rm c}} \frac{{\rm d}Q}{Q}\left(\frac{1+8Q^4-8Q^2}{1-Q^2}\right)\frac{1}{\rho(k,k')} \times \{C(k,k')\cos[\eta(k,k')] - D(k,k')\sin[\eta(k,k')]\}. \quad \text{(A.28)}$$

The functions C, D, η and ρ are precedently defined.

References

1. A.B. Migdal, Zh. Eksp. Teor. Fiz. **34**, 1438 (1958) [Sov. Phys. JETP **7**, 996 (1958)].
2. G.M. Eliashberg, Zh. Eksp. Teor. Fiz. **38**, 966 (1960) [Sov. Phys. JETP **11**, 696 (1960)].
3. J.P. Carbotte, Rev. Mod. Phys. **62**, 1027 (1990).
4. Y.J. Uemura *et al.*, Phys. Rev. Lett. **66**, 2665 (1991).
5. O. Gunnarson, Rev. Mod. Phys. **69**, 575 (1997).
6. C. Grimaldi, L. Pietronero, S. Strässler, Phys. Rev. Lett. **75**, 1158 (1995).
7. L. Pietronero, S. Strässler, C. Grimaldi, Phys. Rev. B **52**, 10516 (1995); C. Grimaldi, L. Pietronero, S. Strässler, Phys. Rev. B **52**, 10530 (1995).
8. M. Capone, S. Ciuchi, C. Grimaldi, Europhys. Lett. **42**, 523 (1998).
9. E. Cappelluti, L. Pietronero, Phys. Rev. B **53**, 932 (1996); *ibid.*, Europhys. Lett. **36**, 619 (1996).
10. A. Perali, C. Grimaldi, L. Pietronero, Phys. Rev. B **58**, 5736 (1998).
11. C. Grimaldi, L. Pietronero, M. Scattoni, Eur. Phys. J. B **10**, 247 (1999).
12. D.A. Wollman, D.J. van Harlingen, W.C. Lee. D.M. ginsberg, A.J. Legget, Phys. Rev. Lett. **71**, 2134 (1993); D.A. Brauner, H.R. Ott, Phys. Rev. B **50**, 6530 (1994); C.C Tsuei *et al.*, Phys. Rev. Lett. **73**, 593 (1994); A. Mathay, Y. Gin, R. C. Black, A. Amar, F.C. Wellstood, Phys. Rev. Lett. **74**, 797 (1995).
13. Z.-X. Shen *et al.*, Phys. Rev. Lett. **70**, 1553 (1993).
14. A.I. Lichtenstein, M.L. Kulić, Physica C **245**, 186 (1995).
15. M. Mierzejewski, J. Zieliński, P. Entel, Phys. Rev. B **57**, 590 (1998).
16. R. Fehrenbacher, M.R. Norman, Phys. Rev. Lett. **74**, 3884 (1995).
17. M. Grilli, C. Castellani, Phys. Rev. B **50**, 16880 (1994); R. Zeyher, M. Kúlic, Phys. Rev. B **53**, 2850 (1996).
18. O.V. Danylenko, O.V. Dolgov, M.L. Kúlic, V. Oudovenko, Eur. Phys. J. B **9**, 201 (1999).